Supporting information:

Thermodynamic characterization of amyloid polymorphism by Microfluidic Transient Incomplete Separation

Azad Farzadfard [A,1,2], Antonin Kunka [A,1], Thomas Oliver Mason[1], Jacob Aunstrup Larsen[1], Rasmus Krogh Norrild[1], Elisa Torrescasana Dominguez[1], Soumik Ray[1], and Alexander K. Buell[1]*,

[1] Protein Biophysics group, Department of Biotechnology and Biomedicine, Technical University of Denmark, Søltofts Plads, Building 227, 2800, Kgs. Lyngby, Denmark

[2] Interdisciplinary Nanoscience Center (iNANO), Aarhus University, Gustav Wieds Vej 14, 8000, Aarhus C, Denmark

[A] Authors with equal contribution to the work.

*** To whom correspondence should be addressed at alebu@dtu.dk**

SI section 1. On the investigations for intermediate species of αSyn fibrils

We tested whether the soluble, diffusive species is indeed monomeric or includes potential aggregation intermediates such as low molecular weight oligomers, similar to those detected by TDA during aggregation kinetics of amyloid beta peptides [1-3]. Towards this, we re-analyzed the data in three different ways. First, we allowed the size of the soluble species to vary to investigate any potential changes in size as a function of increasing urea concentration (SI Figure S5a). In most cases, we observed fluctuations of the hydrodynamic radius within the range expected for a monomeric sample. The largest differences were observed in samples containing 0 - 2 M urea where the overlap between the transient and Gaussian peaks are the most dominant and, consequently, the parameter correlations the highest. In some cases, the size was below 2 nm corresponding to a small amounts of degradation products detected also using the SDS-PAGE (data are not shown). Second, we a priori assumed that soluble species in Taylor regime consist of different n-mers of synuclein (n = 2, 3, 4, 5 and 10) and fixed the peak variance to the corresponding values during fitting of the elution profiles (SI Figure S6b). The comparison of the goodness-of-fits in terms of R^2 revealed that the discrimination between different sizes of soluble species is difficult (SI Figure S5c). The monomeric species fitted best the depolymerization data of fibrils made in the presence of KCl (polymorph S), whereas a clear distinction between monomers, dimers, and trimers could not be made in case of the other fibril types (SI Figure S5c). Third, we assumed a situation where the soluble species are mixtures of monomers and higher oligomers. Towards this, we introduced additional parameters during fitting of the depolymerization series to account for the presence of a third species (with R_h in range of 4-9 nm expected to be in the Taylor regimes based on our simulations, SI Figure S1). Although some data points indicated the presence of oligomers (SI Figure S5d), a closer scrutiny of the fittings revealed uncertainties primarily due to the over parameterization. Furthermore, no improvement in the residuals of individual fits was observed upon introduction of the additional species. Finally, to fully confirm our assumption regarding the monomeric nature of the soluble species, we analyzed the supernatants of fibrils equilibrated at 0, 1, and 2 M urea using FIDA and DLS (SI figure S6 and SI table S3). The average hydrodynamic radius obtained by both methods was 3.2 nm corresponding to αSyn monomer which, together with the analyses described above, fully justifies the two-state approximation of the fibril depolymerization. However, such scenario might not be true for other amyloid systems [1-3] and additional experiments such as the ones described here should be carried out to investigate presence and fraction of any on-pathway oligomeric species. Consequently, we advocate to use the minimal two-species fit to obtain reliable quantification of soluble species and verify presence of oligomeric species via an alternative technique.

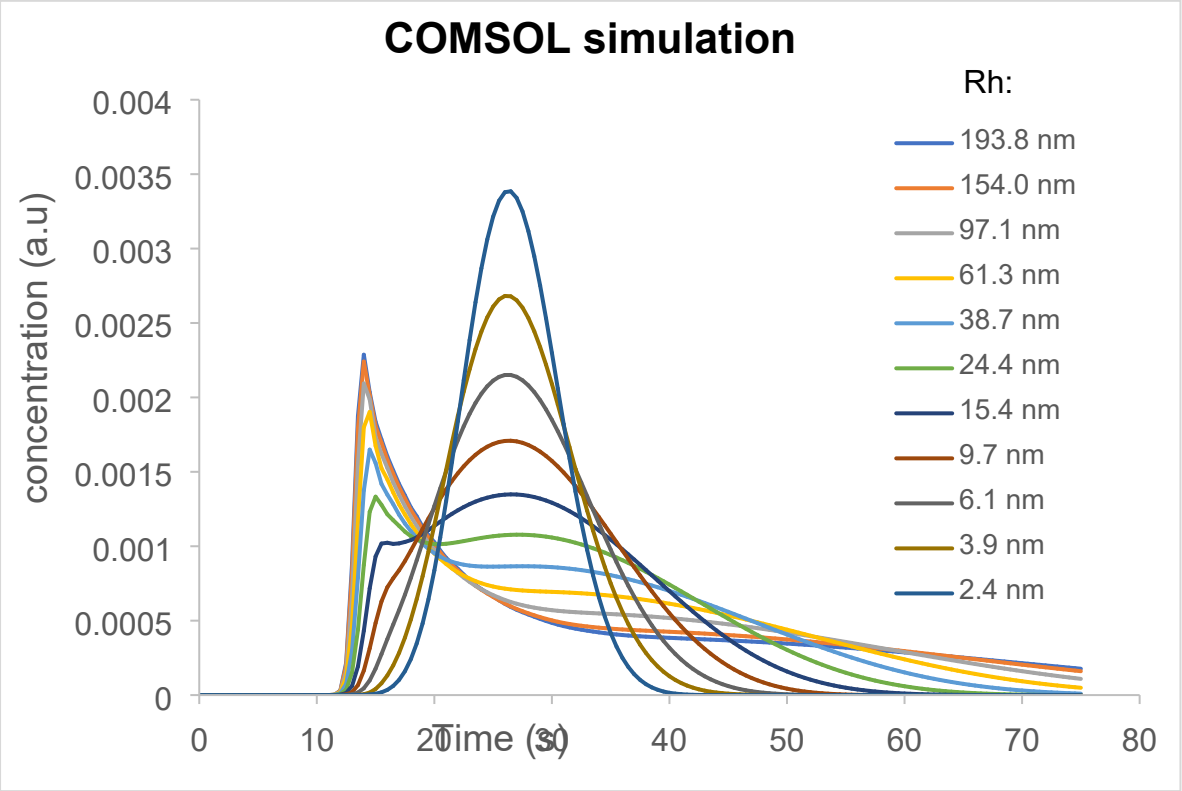

SI figure 1. COMSOL simulation for different particle sizes from 2.4 nm to 193.8 nm hydrodynamic radius in FIDA similar to our experimental setup i.e, injection of an initial plug (75 mbar, 20 s) followed by 75 s experiment run with 1500 mbar.

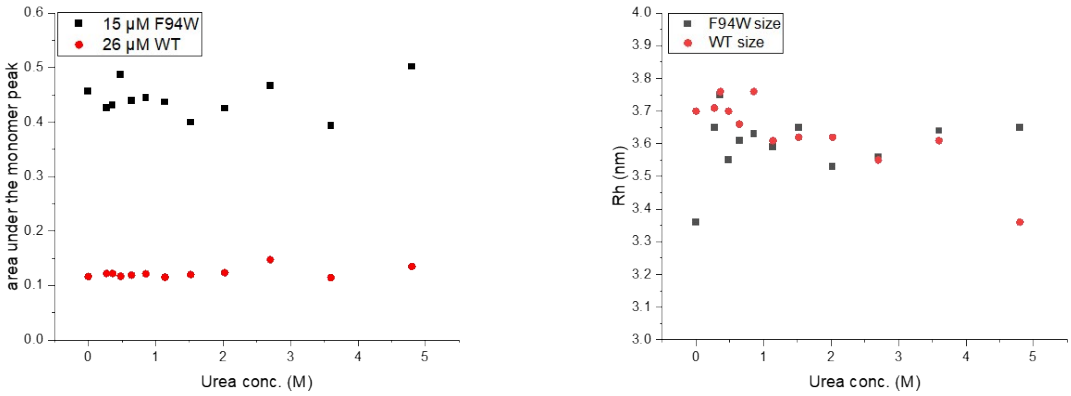

SI figure 2. FIDA fluorescent signal for WT and F94W αSyn is independent of the urea concentration. The injected plug contains αSyn monomer in different concentrations of urea (0 to 4.8 M). Integrated area under the monomer peak (left panel) and the monomer size obtained by FIDA (right panel) show insignificant changes in different urea concentrations.

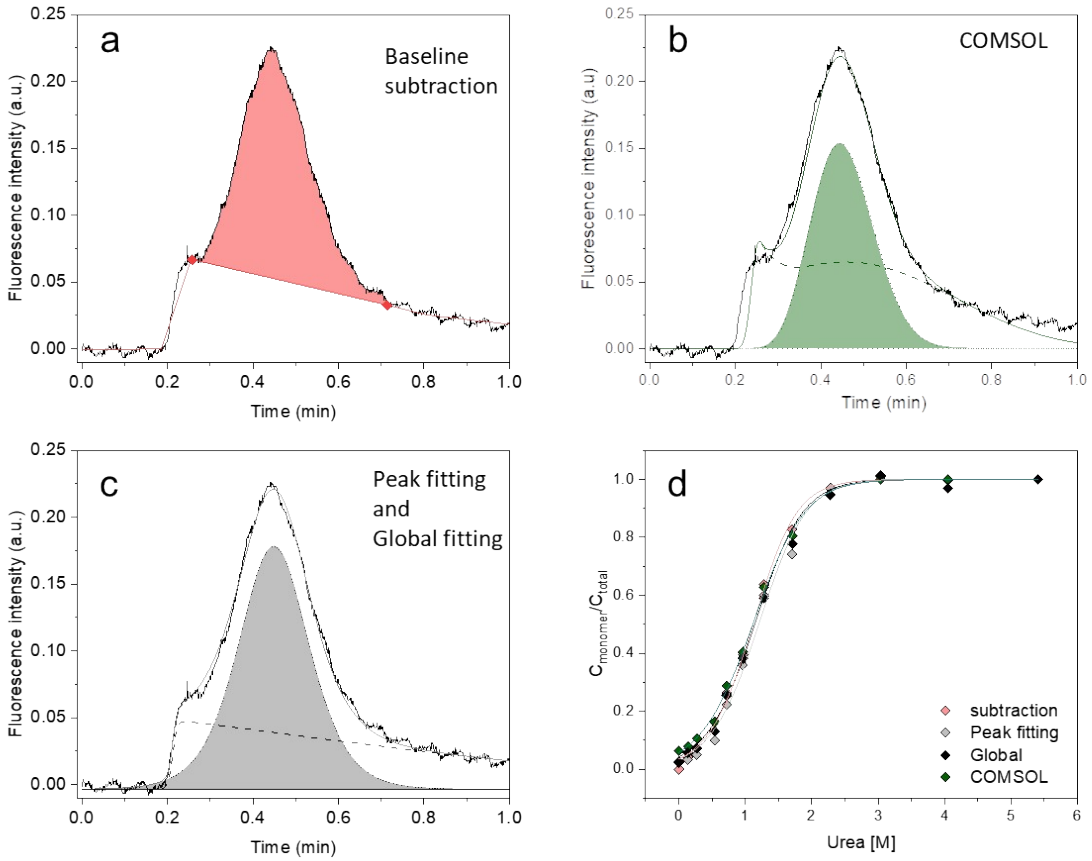

SI figure 3. Deconvolution and quantification of monomer peak in FIDA experiments. The area of the monomer peak was obtained for the sample equilibrated in 1 M urea by (a) baseline subtraction, (b) COMSOL simulations, and (c) fitting the whole curve with a composite equation of normal and skewed Gaussian either for individual curves independently or globally in the context of the isodesmic linear polymerization model. (d) The normalized data obtained by different deconvolution methods are plotted together. Lines are independent isodesmic fits to the points in the corresponding colour. Values of ΔG, the thermodynamic stabilities of the fibrils, are provided in SI table 1.

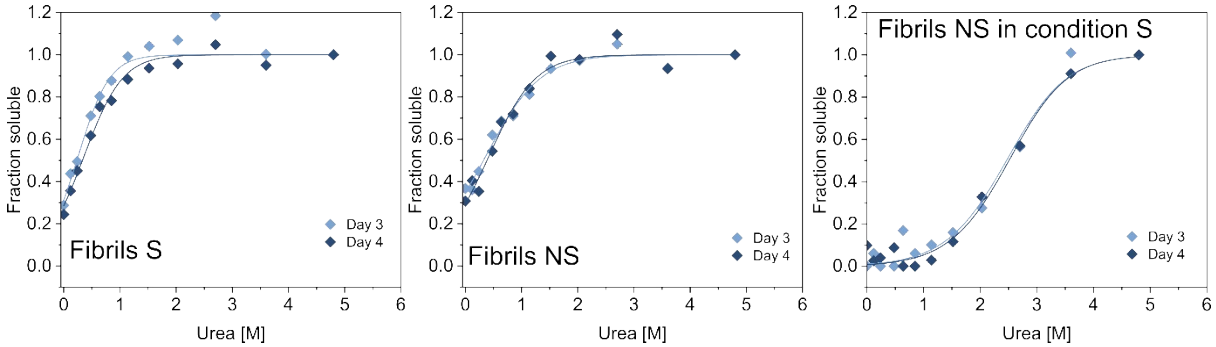

SI figure S4. Comparison of urea depolymerization curves after 3 and 4 days for α-Syn polymorphs S (left panel) and NS in NS condition (middle panel) and S condition (right panel). The similar curves show that the components are already in equilibrium.

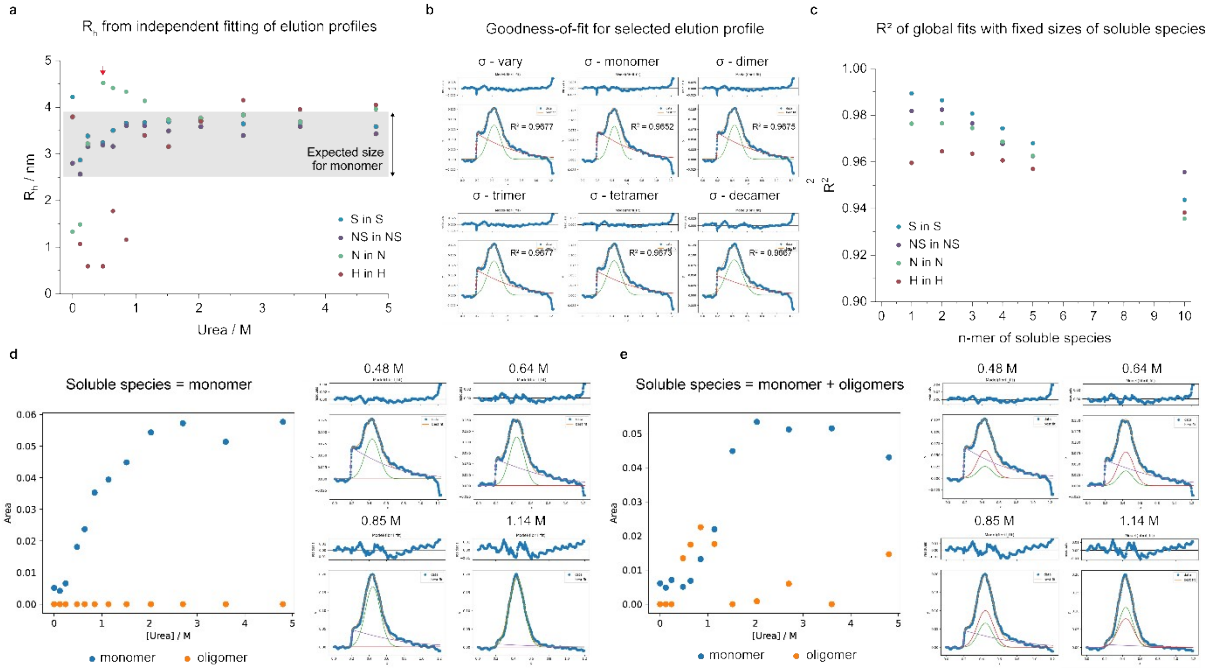

SI Figure S5: Analysis of the oligomeric state of the soluble species during TIS. a) Size variation of the soluble species as a function of urea for different fibril types. The elution profiles were fitted individually to the sum of equations 9 and 10 using an in-house written python script**. b) Analysis of the selected elution profile (fibrils N measured at 0.48 M urea, marked by a red arrow in a) assuming different size of the oligomeric species.** The variance of the Gaussian peak was fixed to the values corresponding to R_h expected for different n-mers under the given experimental conditions. **c) Comparison of the R^2** for fits of elution profiles measured at 0.48M urea for different fibrils. **d) Area of the monomer peak as a function of urea** obtained by the independent fitting of elution profiles of fibril N using the three-species function (single transient and two Gaussian functions) with the area of the third species fixed to 0. Examples of 4 elution profiles are shown on the right. **e) Areas of the monomer and oligomer peaks as a function of urea** obtained by the independent fitting of elution profiles of fibril N using the three-species function (single transient and two Gaussian functions) with the variance of the third species fixed to number corresponding to different n-mer sizes (n=2-5). Examples of 4 elution profiles are shown on the right. No change in the oligomer areas (orange) was observed for different oligomer sizes.

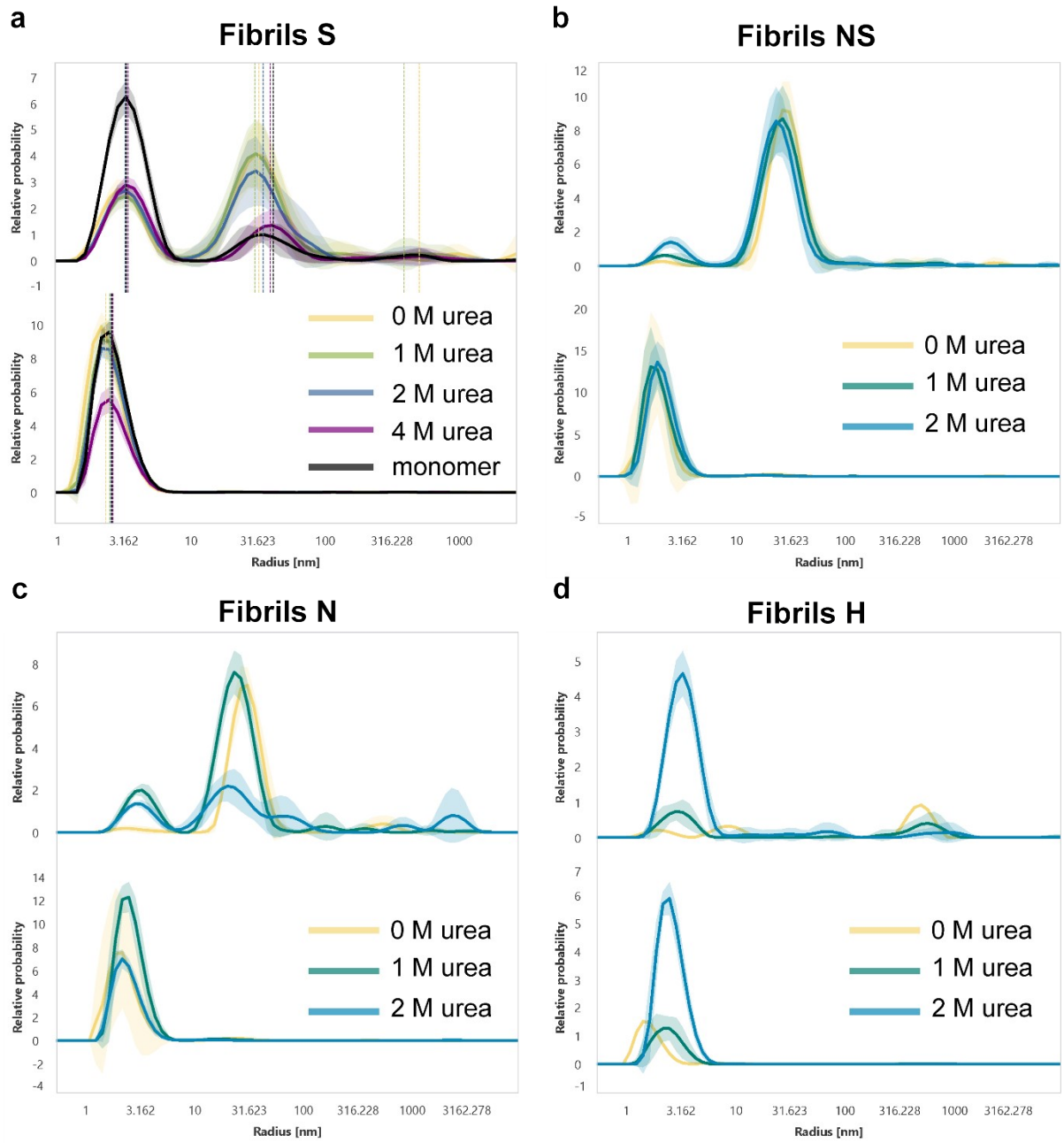

SI Figure S6: DLS analysis of the soluble fractions. Fibrils S (a), NS (b), N (c), and H (d) were equilibrated in 0, 1, and 2 M urea and centrifuged. The plots show results of the size distribution fits to the DLS correlation functions collected for the supernatants. The top and bottom subplots depict the intensity and mass weighted distribution of species, respectively. Based on their comparison we conclude that higher oligomeric or small fibrillar species can be present, albeit in < 0.1 % abundance. The results of size distribution fits are provided in SI table S3.

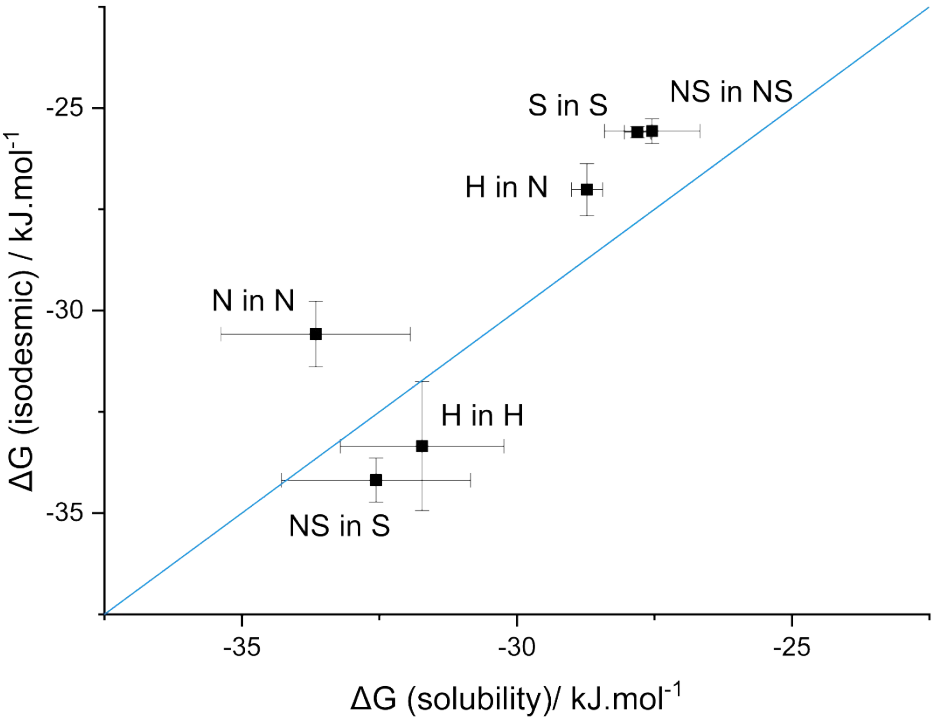

SI Figure S7: Comparison of the ΔG values obtained from fitting the depolymerization data with the isodesmic model (y-axis) and those calculated from the concentration of the monomer in the absence of urea directly determined and converted into free energies using equation 2. The monomer concentrations and corresponding ΔG values were calculated from the points at 0 M urea in Figure 4. The blue line indicates a line of slope 1.0.

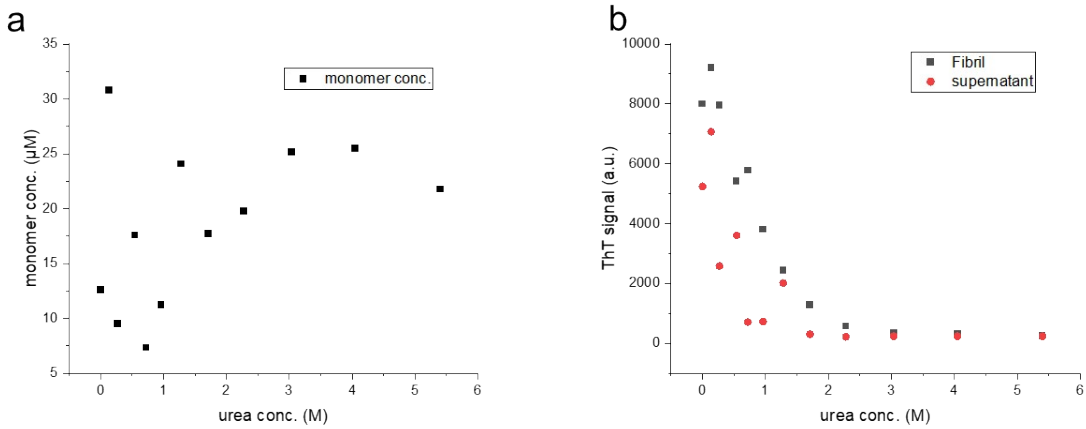

SI figure S8. Ultracentrifugation failed to separate sonicated αSyn fibrils from monomer. (a) concentration of αSyn monomer in supernatant after 180000 g ultracentrifugation for 2 hours measured by 280 nm absorption with a Nanodrop instrument. The scattered absorption data suggest the presence of small aggregate species that can scatter the light 280. (b) The supernatant was still ThT positive after the ultracentrifugation.

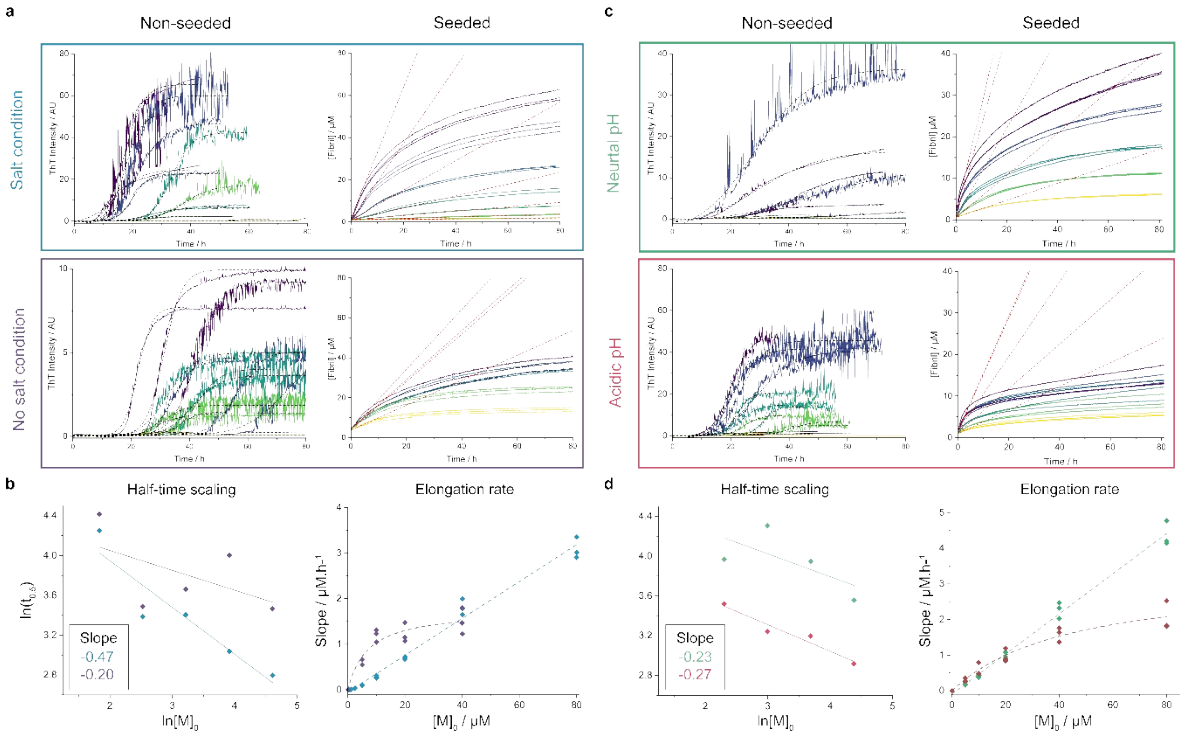

SI figure S9. Kinetics of αSyn fibril formation in different conditions. (a, b) condition S (150 mM KCl, 50 mM Tris pH 7.5) show faster aggregation than condition NS (5 mM Tris pH 7.5) and c, d) condition H (150 mM NaCl, 20 mM acetate pH 5) lead to faster aggregation in comparison to conditions N (150 mM NaCl, 20 mM phosphate pH 7.4). (a) and (c) the aggregation profile with different concentrations of monomer monitored in a time course either in unseeded (left panels) or in seeded (right panels) experiments. Dashed lines show logistic fits (see materials and methods section) in unseeded experiments to obtain $t_{0.5}$ and linear fit to the first 5 hours of the curves in seeded experiments to obtain apparent elongation rates. (b) and (d) represent the fitted value against the monomer concentration in log-log plot for unseeded (left panels) and linear scale for seeded experiments (right panels). (b) blue and purple curves represent S and NS conditions, (d) green and red curves represents N and H conditions.

SI table S1: ΔG values obtained by isodesmic fits for the data points extracted with different deconvolution methods from the same FIDA curves for F94W αSyn fibril depolymerization assay.

Method	ΔG (kJ.mol^{-1})	m* (kJ.M^{-1}.mol^{-1})	R^2
Baseline subtraction	-34.6 ± 0.36	8.15 ± 0.34	0.998
Peak fitting	-34.64 ± 0.56	7.60 ± 0.48	0.995
Global peak fitting	-34.08 ± 0.03	7.51 ± 0.01	0.980
COMSOL	-33.18 ± 0.22	6.92 ± 0.20	0.999

SI table S2: ΔG values obtained from the isodesmic fitting of the urea depolymerization in day 3 and 4. Data points and curves are shown in SI figure S4.

The fibril type	Day 3		Day 4	
	ΔG ($kJ.mol^{-1}$)	**m** ($kJ.M^{-1}.mol^{-1}$)	**ΔG** ($kJ.mol^{-1}$)	**m** ($kJ.M^{-1}.mol^{-1}$)
S	-25.9 ± 0.4	9.4 ± 0.1	26.3 ± 0.3	7.6 ± 0.6
NS	-25.5 ± 0.3	5.4 ± 0.5	-26.2 ± 0.4	6.3 ± 0.7
NS in S condition	-37.5 ± 1.4	5.5 ± 0.6	-37.7 ± 1.4	5.6 ± 0.6

SI Table S3: Analysis of the soluble fractions of different fibrils in various urea concentrations. Fibrils S (a), NS (b), N (c), and H (d) were equilibrated in 0,1, and 2 M urea were centrifuged, and the respective supernatants analyzed using FIDA and DLS. The results of DLS are shown in SI Figure S7. PDI – polydispersity index

		FIDA	DLS					
		Species 1	Peak 1 (nm)		Peak 2 (nm)		Peak 3 (nm)	
fibril	urea [M]	Rh (nm)	mean	PDI	⌀	PDI	⌀	PDI
A	0	2.77	3.03	0.09	29.54	0.1	2107.2	0.02
	1	2.82	3.32	0.09	29.95	0.11	312.66	0.04
	2	3.45	3.35	0.09	30.76	0.15	167.64	0.05
B	0	3.47	3.15	0.04	29.72	0.14	183.01	0.03
	1	3.03	2.3	0.05	27.73	0.45	-	-
	2	2.91	2.78	0.07	24.02	0.12	515	0.03
N	0	2.91	3.38	0.02	30.45	0.08	609.97	0.04
	1	2.97	3.66	0.14	25.34	0.2	618.86	0.06
	2	3.53	3.32	0.22	22.09	0.26	1831.53	0.03
H	0	< 2	4.35	0.01	-	-	465.98	0.02
	1	< 2	3.27	0.07	-	-	626.12	0.05
	2	2.69	3.27	0.08	70.14	0.06	653.22	0.1

References:

1. Deleanu, M.; Deschaume, O.; Cipelletti, L.; Hernandez, J. F.; Bartic, C.; Cottet, H.; Chamieh, J., Taylor Dispersion Analysis and Atomic Force Microscopy Provide a Quantitative Insight into the Aggregation Kinetics of Abeta (1-40)/Abeta (1-42) Amyloid Peptide Mixtures. *ACS Chem Neurosci* **2022,** *13* (6), 786-795.
2. Deleanu, M.; Hernandez, J. F.; Cipelletti, L.; Biron, J. P.; Rossi, E.; Taverna, M.; Cottet, H.; Chamieh, J., Unraveling the Speciation of beta-Amyloid Peptides during the Aggregation Process by Taylor Dispersion Analysis. *Anal Chem* **2021,** *93* (16), 6523-6533.
3. Deleanu, M.; Hernandez, J. F.; Cottet, H.; Chamieh, J., Taylor dispersion analysis discloses the impairment of Abeta peptide aggregation by the presence of a fluorescent tag. *Electrophoresis* **2023,** *44* (7-8), 701-710.